A Low-Profile Frequency Reconfigurable Grid-Slotted Patch Antenna

Yuan-Ming Cai[1], (Member, IEEE), Ke Li[2], (Member, IEEE), Yinzeng Yin[1], Steven Gao[3], (Senior Member, IEEE), Wei Hu[1], (Member, IEEE), Luyu Zhao[1], (Member, IEEE)

[1]National Key Laboratory of Antennas and Microwave Technology, Xidian University, Xi'an, Shaanxi, 710071, China
[2]School of Information Science and Technology, Northwest University, Xi'an, Shaanxi, 710127, China
[3]School of Engineering and Digital Arts, University of Kent, Canterbury CT2 7NT, U.K

Corresponding author: Yuan-Ming Cai (ymcai@xidian.edu.cn), Ke Li(like@nwu.edu.cn).

This work was supported in part by the China Postdoctoral Science Foundation under Grant 2016M602769, the Fundamental Research Funds for the Central Universities under Grant JBX170215, and the National Natural Science Foundation of China (No. 61501340 and No. 61701366).

ABSTRACT This paper presents a novel low-profile high gain frequency reconfigurable patch antenna with unidirectional radiation pattern by using a grid-slotted patch with tunable varactors loading. The antenna consists of two stacked substrates and three metal layers. A grid-slotted patch with two tunable varactors is placed on the top layer, a microstrip line is placed in the middle of two substrates, and the ground plane is on the bottom layer. A single DC voltage applied on two varactors is used to control the working frequencies of the proposed antenna. By altering the bias voltage, the working frequency of the proposed antenna can be continuously changed within a wide range from 2.45 GHz to 3.55 GHz. The antenna maintains broadside radiation and stable radiation pattern in all the operating modes. The measured antenna gain of the proposed antenna rises from 4.25 dBi to 8.49 dBi with the working frequency increases from 2.45 GHz to 3.55 GHz. Compared to other frequency-reconfigurable antennas available in the literature, the proposed antenna has advantages of a wide frequency tuning range over a bandwidth of 1.45:1, high frequency selectivity, low profile (0.016 free space wavelength at 2.45 GHz), high gain, stable unidirectional pattern, simple structure, and low cost. These advantages make it a promising candidate for cognitive radio and future wireless communication systems.

INDEX TERMS Continuously tuning, frequency reconfigurable antenna, varactors.

I. INTRODUCTION

Recently, frequency reconfigurable antennas have obtained increasing attention because they are in great demand for a variety of multiple frequency systems and cognitive radio systems which can improve spectrum efficiency [1]. Good frequency selectivity, stable radiation patterns, and wide frequency tuning range are desired for frequency-reconfigurable antennas. Meanwhile, with small size, low-profile, simple structure, and low cost, frequency reconfigurable antennas can be easily integrated in the wireless system.

Physically reconfigurable antennas [2, 3] and electrically reconfigurable antennas [4-6] are two major types of frequency reconfigurable antennas [7]. Despite the advantages of low insertion loss and high reliability, the physically reconfigurable antennas, also known as mechanically reconfigurable antennas, are difficult to tune and hardly applied in fast time varying control [8]. Electrically reconfigurable antennas based on the use of electrically controlled devices are desired in many applications due to high switching speed, simple structure and relatively low price.

Tunable varactors, tunable materials and switches including RF-MEMS switches and PIN diodes are usually used to design electrically frequency reconfigurable antenna [9]. Various microstrip reconfigurable antennas have been applied as they have advantages of low cost, low profile and ease of fabrication [10-16]. In [10], five RF p-i-n diode switches are placed on a slot under a microstrip patch antenna to achieve frequency reconfigurable between nine discrete bands. The microstrip patch antenna is switched to slot antenna as the operational frequency decreases. In [11], a four states frequency reconfigurable antenna is reported by loading three PIN diode switches on the radiation patch of a compact microstrip antenna. By changing the states of the switches, the four different resonant frequencies are obtained. A microstrip slot antenna using the RF MEMS switches have been presented to achieve operating frequency band changing

between 2.45 GHz and 5.2GHz [12]. One common problem for these reconfigurable antennas based on switches is that the working frequency cannot be tuned continuously. The switch elements providing the ON/OFF functions only facilitate fixed band, therefore, those antennas cannot obtain a frequency-agile property to continuously shift the operational bands across the entire sensing band.

A continuously frequency tunable antenna is reported in [14]. A trimmer is used to control the operational frequency of a microstrip antenna. The trimmer, acting as a tunable capacitor soldered to the microstrip feed line, needs to be rotated manually to change the capacitance. The working band can be altered continuously from 2.6 GHz to 3.35 GHz, translating into a 1.28 reconfigurable frequency ratio. By loading ferroelectric varactors along a slot loop, a frequency-reconfigurable antenna is designed [15]. The reconfigurable frequency ratio is 1.36. The gain of the antenna is lower than -3 dBi due to the very compact size of antenna and loss of the FE varactors. A slot antenna with two varactor is reported in [17] and the simulated result shown a wide tuning range of 1.56:1. Due to the omnidirectional radiation pattern, the peak gain of the antenna is from 1.1 to 2.4 dB. Wideband dipole antenna or monopole antenna mounted above an active FSS reflector has been presented to achieve the continuous frequency tuning in [18, 19]. Due to the in-phase reflection of the FSS, the backward radiation can be avoided and the profile of the antenna can be reduced dramatically. However, a large physical length is usually required to obtain a tunable FSS reflector.

The design of microstrip patch antennas with varactors is studied previously in [20-22]. The operational bands of the frequency reconfigurable antennas are controlled by the biasing voltages of the varactors. The reconfigurable frequency ratios of the tunable operational frequencies in [20] and [21] are 1.1 and 1.33, respectively. To further extend the tunable range of the microstrip patch antenna, a dual-band stacked patch antenna with air substrate is presented in [22], and the two working frequencies can be continuously tuned within two bands from 1.68 to 1.93 GHz and from 2.11 to 2.51 GHz.

In 2014 and 2015, metamaterial-based grid-slotted mushroom antenna and microstrip patch antenna are extensively reported in [23-26]. The grid-slotted patch can be excited by slot patch. By using arrays of sub-wavelength patches, the grid-slotted microstrip patch antennas show advantages of high gain, low-profile and wide operational band. This phenomenon can be considered as the effects of surface waves propagating on the finite-sized RIS-based antennas [25]. Frequency reconfigurable operation was also presented in several research papers based on the concept of the grid-slotted microstrip patch antenna [27-30]. However, those reconfigurable antennas are mechanically reconfigurable antennas.

In this paper, a low-profile grid-slotted frequency reconfigurable antenna is proposed based on our previously published conference paper [31]. In the conference paper, antenna structure and preliminary simulation results are presented. In this paper, the prototype of the proposed antenna is fabricated and measured, and further analysis and experimental results are given in details. The antenna consists of two stacked substrates with the thickness of 1 mm. The profile of the proposed antenna is only 2 mm. A grid-slotted patch with tunable varactors is placed on the top layer. By controlling the capacitance of the varactors, the resonant frequency of the antenna can be continuously tuned in a wide range from 2.45 to 3.55 GHz. High frequency selectivity is obtained. Furthermore, the unidirectional radiation pattern of the antenna at its tunable resonant frequency stays stable, and a good gain, varying from 4.25 dBi to 8.49 dBi, can be observed within the wide tuning band. Very simple DC biasing circuit is designed to control the varactors and a single voltage is enough for antenna frequency tuning.

II. ANTENNA GEOMETRY

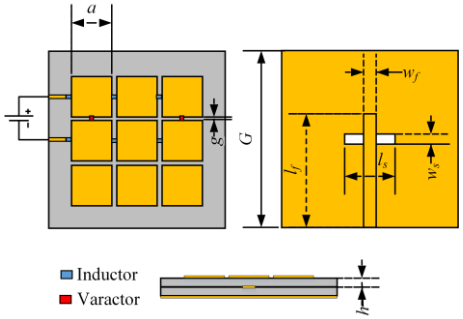

FIGURE 1. The geometry of the proposed antenna (a = 18 mm, g = 0.4 mm, l_s = 20 mm, l_f = 42.5 mm, w_f = 3 mm, w_s = 3 mm, G = 70 mm).

The proposed antenna consists of three metal layers separated by two square F4B substrates with size of 70 × 70 mm^2, relative permittivity of 2.2, loss tangent of 0.002, and thickness of 1 mm as shown in Fig. 1. The two substrates are stacked together closely and there is no air gap between the substrates. A grid-slotted patch works as a radiator is printed on the top layer. The patch is divided into 3×3 small patches by two horizontal slots and two vertical slots. The size of each small patch is $a \times a$, and the width of the slots is g. A microstrip feeding line is placed in the middle of the substrates with the width of W_f and length of L_f. A metallic ground plane with a rectangle aperture-coupling slot etched on is printed on the bottom layer. The length of the slot is Ls and the width of the slot is W_s. As shown in Fig. 1, two varactors are applied on the grid slot patch for frequency reconfigurability. The varactor diodes are SMV1405 from Skyworks where the capacitance of the diodes changes from 2.67 pF to 0.63 pF when the reverse bias voltage increases from 0 V to 30 V [32]. The cathodes of the varactors are soldered to the patches in the first row and the anodes of the varactors are soldered to the patches in the second row. The gaps between three patches in the first row are bridged by two inductors which is placed at the center of edges, and gaps

between three patches in the middle row are bridged by two inductors as well. Those four inductors with the inductance of 33 nH are used in this design to build the DC biasing circuit. The patches in the first row or in the second row are shorted for DC current and isolated from RF signal by the inductors. Two DC lines are connected to the patches in the first row and patches in the second row with 33 nH inductor chocks to achieve AC/DC isolation. By doing so, the DC voltage can be applied on the varactors in parallel through two DC lines, and only a single voltage between the DC lines is required to control the varactors.

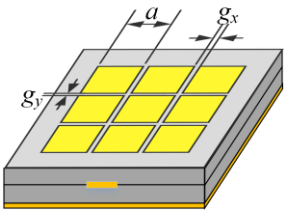

FIGURE 2. The structure of the analyzed grid-slotted patch antenna.

III. Antenna Design and Theory

The reconfigurable antenna is based on the study of a grid-slotted patch antenna. The first step to implement the proposed reconfigurable antenna is the design and the investigation of a grid-slotted patch antenna as shown in Fig. 2. The grid-slotted patch antenna in Fig. 2 is a microstrip fed aperture-coupled patch antenna. The radiation patch consists of an array of 3×3 periodically arranged square patches. As the effects of surface waves propagating on the finite-sized grid-slotted patches array, the antenna can work effectively with higher gain. The analysis and modeling of the surface wave resonances on RIS-based antenna were presented theoretically and computationally in [33]. The detail design principle of the grid slotted patch excited with an aperture-coupling feeding technique is also described in [24], which is the basis of the work. The corresponding antenna performance is to be analyzed by considering the dispersion property of the capacitor-loaded patch unit cell. The cavity model is applicable to the mode analysis of the grid slotted patch antenna. By considering the finite-sized capacitor-loaded patches as a cavity, the surface wave resonance can be qualitatively determined by the following equation (1).

$$\beta = \frac{\pi}{L_{cav}} \tag{1}$$

Where the β respects the propagation constant of the surface wave mode and the L_{cav} is the length of the cavity which can be calculated by the number of unit cells N multiplied by the cell periodicity (a+g). The dispersion diagram of the HIS structure can be calculated with the linked boundary condition by using the HFSS software.

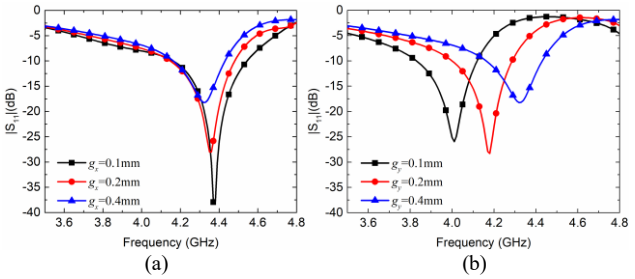

FIGURE 3. Simulated $|S_{11}|$ with different values of g_x and .g_y

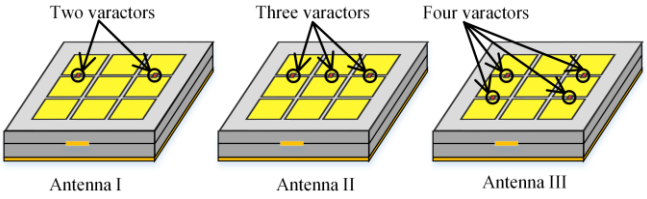

FIGURE 4. Antennas with loading varactors.

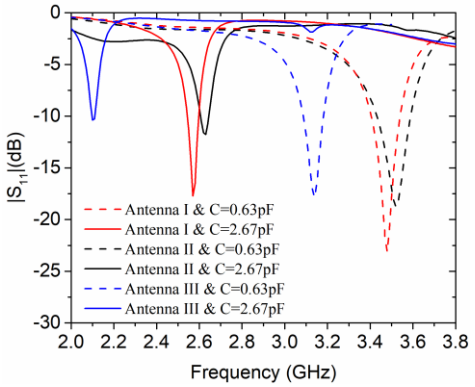

FIGURE 5. Simulated $|S_{11}|$ with different loading varactors.

A grid slot antenna is analyzed firstly, as shown in Fig. 2. The simulated $|S_{11}|$ of the analyzed grid-slotted patch antenna with different values of g_x and g_y are presented in Fig. 3. It can be seen that, the value of g_y influence the resonant frequency significantly, while the value of g_x can slightly affect the resonant frequency. The width of the radiating slot g_y, which determines the capacitance between adjacent patches, can significantly influence propagation constant of the surface wave, result in resonant frequency shifting. It can be seen that by decreasing the width of the horizontal slot g_y, the equivalent capacitances across the adjacent patches increase and the resonant frequency of the antenna shifts toward lower frequencies. The simulated results indicate that the resonant frequency can be altered by changing the value of the distributed capacitances introduced by the horizontal gap. Therefore, by loading additional capacitors between patches can tune the working frequency of the grid-slotted patch antenna. To verify our concept, the antennas loaded with varactors on horizontal slots, acting as tunable capacitors are studied. The SMV1405 varactor is selected, due to its low series resistance and adequate range of junction

capacitance from 0.63 pF to 2.67 pF. A series RLC equivalent circuit was utilized to model the varactors. The model consists of diode parasitic inductance (L_s=0.7 pF), parasitic resistance (R_s=0.8Ω), and junction capacitance (C_j).

To optimize the location and the number of tunable capacitors, three kinds of antennas integrated with varactors at different locations as illustrated in Fig. 4 are simulated. The simulated $|S_{11}|$ with different values of capacitances of the varactors is shown in Fig. 5. It can be seen that antenna I, antenna II, and antenna III have tunable working frequency. The frequency tuning ranges of the antenna I, antenna II, and antenna III are from 2.57 GHz to 3.48 GHz (red lines in Fig. 5), from 2.62 GHz to 3.51 GHz (black lines in Fig. 5), and from 2.11 GHz to 3.14 GHz (blue lines in Fig. 5). The tuning ranges of those three antennas are similar except for frequency shift. Antenna I has less number of varactors compared with antenna II and antenna III which leading to a lower cost and simple biasing circuits. To make the proposed frequency reconfigurable antenna be cheaper and more simple, we finally choose the antenna I which has only two tunable capacitors. In addition, two capacitors in antenna I is sufficient to control the resonant frequency of the antenna within a wide range.

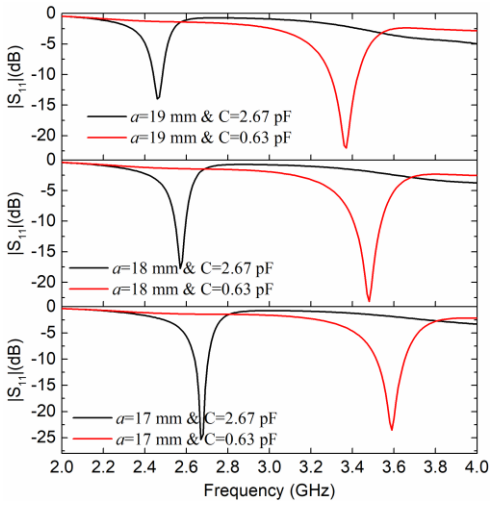

FIGURE 6. Simulated $|S_{11}|$ with different values of a.

The simulated $|S_{11}|$ curves of Antenna I with different values of *a* are plotted in Fig. 6. When the side length of the square patch *a* increases from 17mm to 19 mm, the resonant frequency of antenna I with 0.63 pF capacitance loading shifts from 3.59 GHz to 3.37 GHz and while the resonant frequency with 2.67 pF capacitance loading shifts from 2.67 GHz to 2.46 GHz. It indicates that the tunable frequency band is influenced significantly by the size of the square patch. The simulation results also show that the value of *a* can hardly change the bandwidth of the tunable frequency. The value of *a* is chosen to be 18 mm in our design example.

The design of the frequency reconfigurable antenna is based on the antenna I shown in Fig. 4. Two SMV1405 tuning varactors are used to realize the tunable capacitors loading. The voltage-dependent capacitances of varactors are used to tune the frequency of the antenna. Six inductors are used to provide biasing DC current path. Therefore, a single DC voltage is applied on the varactors in parallel. The capacitance of the varactors changes from 2.67 pF to 0.63 pF when the reverse bias voltage increases from 0 V to 30 V, while the working frequency of the reconfigurable antenna can be shifted continuously.

IV. Simulated and Measured Results

A prototype of the antenna as depicted in Fig. 7 was fabricated to verify our design concept. Two SMV1405 varactors with SC-79 package and six Murata inductors were used. The simulation results are obtained by using the full wave simulation software CST. The S-parameters were measured with the KEYSIGHT E5080A vector network analyzer. The antenna gain and radiation patterns were evaluated in an anechoic chamber using the Satimo SG 24 spherical near-field antenna measurement system.

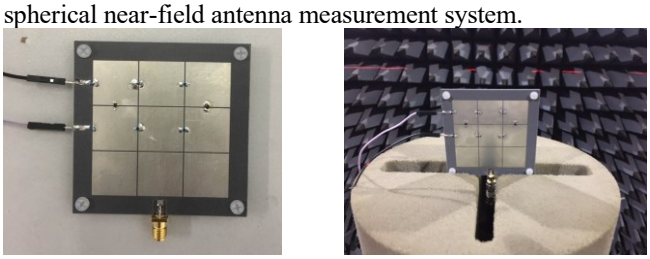

(a) (b)

FIGURE 7. The prototype of the proposed frequency reconfigurable antenna.

A. Impedance Matching

The simulated and measured $|S_{11}|$ of the proposed antenna with respect to six different capacitances or reverse biasing voltages of varactors are superposed in Fig. 8. Reasonable agreement between simulation and measurement is obtained. Table I listed the six operational bands and bandwidths with six different reverse biasing voltages applied. The simulated and measured results show that by altering the capacitances of the varactors on the grid-slotted patch, the resonant frequency of the antenna is shifted continuously. The working band moves toward high frequency with the decrease of capacitances. Good impedance matching is observed and the measured bandwidth (BW) is about 3 % at each band. Although only six operational states within the continuous tuning range is given, the characteristic of continuously frequency reconfigurable can be expected. The center operational frequency varies from 2.45 GHz to 3.55GHz as the reverse biasing voltage increase from 0 V to 30 V.

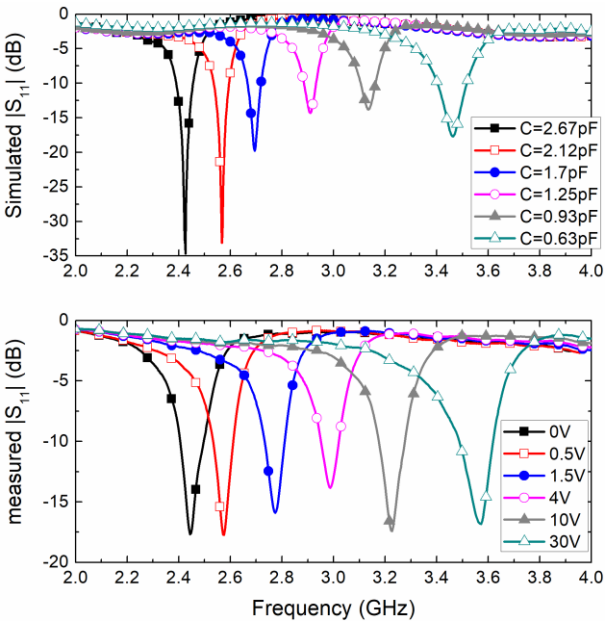

FIGURE 8. Simulated $|S_{11}|$ with respect to different capacitance of varactors.

TABLE 1. Simulated and Measured Working Bands

Antenna state	Band 1	Band 2	Band 3	Band 4	Band 5	Band 6
Biasing voltage, V	0	0.5	1.5	4	10	30
capacitance, pF	2.67	2.12	1.7	1.25	0.93	0.63
Mea. Resonant Freq., GHz	2.45	2.57	2.77	2.99	3.23	3.55
Sim. Resonant Freq., GHz	2.42	2.57	2.69	2.91	3.14	3.46
Mea. BW ($\|S_{11}\|$<-10dB), %	3.77	3.05	2.82	2.34	3.11	3.69
Sim. BW ($\|S_{11}\|$<-10dB), %	2.70	2.30	1.97	1.62	1.85	3.30

B. Gains and Antenna Efficiency

Fig. 9 shows the measured broadside gains-frequency curves of the antenna with six biasing voltages. It can be seen that the proposed antenna has good frequency selective characteristic. The measured peak gain rises from 4.25 dBi to 8.49 dBi as the operational frequency increases from 2.45 GHz to 3.55 GHz. The gain fluctuation is on one hand due to the electrical size of the antenna aperture changed as the free space wavelength is different at different frequency. At lower frequency, the electrical size of the antenna is smaller than that at higher frequency which causes gain drop. On the other hand, the gain fluctuation can be attributed to the different radiation efficiency at different frequencies.

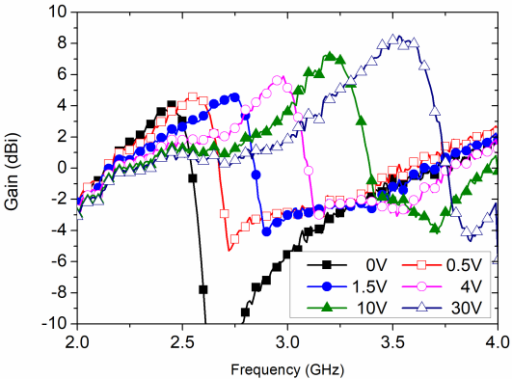

FIGURE 9. Measured antenna gain with respect to different biasing voltage.

TABLE 2. Measured Gains and Efficiency

Antenna state	Band 1	Band 2	Band 3	Band 4	Band 5	Band 6
Sim. Resonant Freq., GHz	2.42	2.57	2.69	2.91	3.14	3.46
Sim. Gain, dBi	4.26	4.94	4.98	5.92	6.91	7.9
Sim. Efficiency	55%	57%	59%	64%	70%	82%
Mea. Resonant Freq., GHz	2.45	2.57	2.77	2.99	3.23	3.55
Mea. Gain, dBi	4.25	4.96	4.74	5.91	7.31	8.49
Mea. Efficiency	49%	54%	50%	60%	78%	90%

The measured efficiencies of the proposed antenna are shown in Table II. The efficiency of the antenna increases from 49 % to 90 % as the resonant frequency increases from 2.45 to 3.55 GHz. The return loss, metal loss, dielectric losses and ohmic losses of varactors contribute to the power loss of the proposed antenna. As the return loss, metal loss and dielectric losses (the loss tangent of the dielectric is 0.002) are negligible compared with the varactors ohmic losses, the ohmic losses of varactors (with series resistance of 0.8 Ω) dominate the power loss of the proposed antenna. The antenna efficiency changes significantly for different DC bias voltage. This is because the current distribution is different at different bands as shown in Fig. 10. When the antenna is operated at a lower frequency (e.g., Band 1), more RF current goes through the varactors compared with that at higher frequency (e.g., Band 6) can be observed. Therefore, ohmic losses of the varactors at lower frequency is more than that at higher frequency. The power loss of varactors leads to antenna efficiency reduction is the common drawback when the varactors are used as tunable capacitors to design reconfigurable antennas [5].

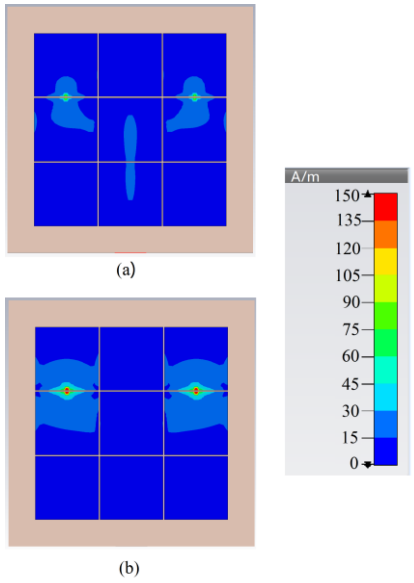

FIGURE 10. **Current distribution of the antenna at different frequency: (a) Band 6 (3.46 GHz); (b) Band 1 (2.42 GHz).**

C. Radiation Pattern

The measured radiation patterns at the measured resonant frequencies of six states with simulated radiation pattern at simulated resonant frequencies are shown in Fig. 11. Good agreement between the simulated results and measured results is obtained. The simulated cross polarization levels are below -30 dB and the measured cross polarization levels are below -20 dB. The measured front-to-rear ratio (F/B) is greater than 10 dB at different states. To sum up, this antenna is unidirectional and the radiation is stable in a wide frequency range.

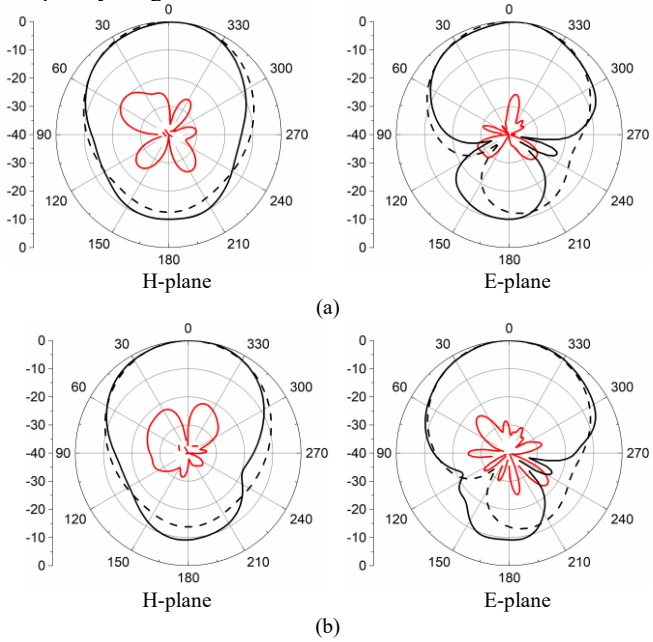

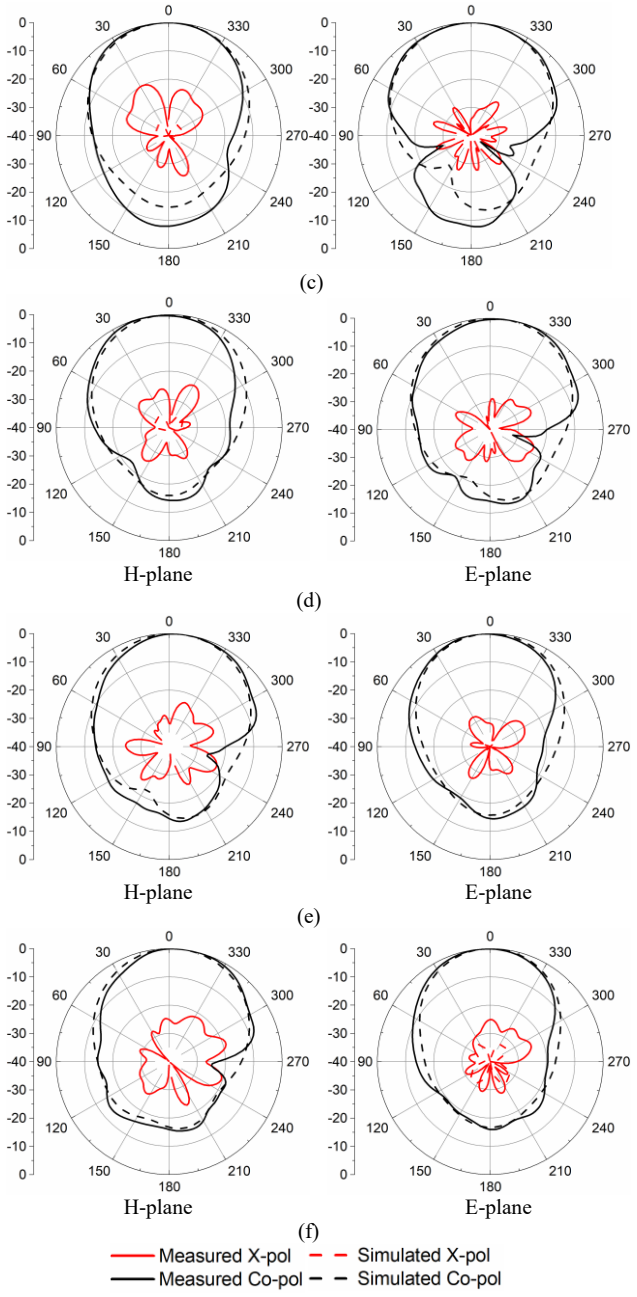

FIGURE 11. **Simulated and measured radiation pattern of different states: (a) Band 1 simulated result at 2.42 GHz and measured result at 2.45 GHz; (b) Band 2 simulated result at 2.57 GHz and measured result at 2.57 GHz; (c) Band 3 simulated result at 2.69 GHz and measured result at 2.77 GHz; (d) Band 4 simulated result at 2.91 GHz and measured result at 2.99 GHz; (e) Band 5 simulated result at 3.14 GHz and measured result at 3.23 GHz; (f) Band 6 simulated result at 3.46 GHz and measured result at 3.55 GHz.**

D. Performance Comparison

Finally, in Table III, performance of the proposed antenna is compared to other continually frequency-reconfigurable antennas [14, 15, 17-22, 27]. Despite its compact size and use of only 2 varactor diodes, the proposed antenna shows

TABLE 3. Performance Comparison of Frequency Reconfigurable Antennas

	antenna types	var. No.	Frequency (GHz)	Tuning Range (%)	Gain (dBi)	Profile (mm)	Size (λ_L)*	reconfigurable mechanism
[14]	Patch antenna with tunable feed network	/	2.6 to 3.35	25.2	Not given	12	1.3×1.3	mechanical
[15]	Slot-loop antenna with ferroelectric varactors	5	6.71 to 9.14	30.7	-3.1 to -5	Not given	0.22 × 0.22	electrical
[17]	Slot-loop antenna with diode varactors	2	2.14 to 3.33	43.5	1.1 to 2.4	0.8	0.29×0.17	electrical
[18]	Dipole antenna with tunable FSS	20	2.26 to 2.75	19.6	3 to 5	5.32	0.6 × 0.6	electrical
[19]	Monopole antenna with tunable FSS	112	1.1 to 1.54	33.3	Not given	10.8	0.63 × 0.63	electrical
[20]	Patch antenna with diode varactors	2	1.92 to 2.1	8.9	-5 to 2	1.6	Not given	electrical
[21]	Patch antenna with diode varactors	1	3.24 to 4.35	29.2	4 to 6.8	3.175	1.08 × 1.08	electrical
[22]	Patch antenna with diode varactors	4	1.68 to 1.93 2.11 to 2.51	13.9 17.3	4.2 to 7.8 4.7 to 7.6	6.17	0.84 × 0.84	electrical
[27]	Rotatable metasurface patch antenna	/	4.76 to 5.51	14.6	5.3 to 5.5	3.048	0.63× 0.63	mechanical
This work	Grid-Slotted Patch Antenna with diode varactors	2	2.45 to 3.55	36.7	4.2 to 8.5	2	0.57 × 0.57	electrical

***λ_L is the free space wavelength at lowest operational frequency**

comparatively better performance including wide frequency tuning range, high gain, unidirectional radiation pattern, low profile, and electrical reconfiguration. In addition, the structure of the proposed antenna is very simple, low cost, and easy to fabricate.

V. Conclusion

A novel low profile frequency reconfigurable grid-slotted patch antenna is proposed in this paper. Two varactors are loaded on the radiation patch to achieve frequency reconfigurablity. Biasing circuits are designed to apply DC voltage on varactors. Only a single DC biasing voltage is used in this design to control the operational frequency of the proposed antenna. A prototype is fabricated and measured. The measured results show that the proposed antenna has a continuously tunable operating frequency ranging from 2.45 GHz to 3.55 GHz by altering the DC voltage applied on the varactors from 0 V to 30 V with an average bandwidth of 3%. The measured radiation patterns are stable within the wide operational frequency range with a good antenna gain from 4.2 to 8.5 dBi. With the low profile, compact size, frequency reconfiguration and stable unidirectional radiation patterns, the proposed antenna can find potential applications for cognitive radio and future wireless communications.

REFERENCES

[1] P. S. Hall, P. Gardner, and A. Faraone, "Antenna Requirements for Software Defined and Cognitive Radios," *Proceedings of the IEEE,* vol. 100, no. 7, pp. 2262-2270, 2012.

[2] M. Weidong, W. Guangming, Z. Bin-feng, Z. Yaqiang, and Z. Xiaofei, "Mechanically reconfigurable antenna based on novel metasurface for frequency tuning-range improvement," presented at the 2016 IEEE International Conference on Microwave and Millimeter Wave Technology (ICMMT), 5-8 June 2016, 2016.

[3] M. N. Pavan and N. Chattoraj, "Design and analysis of a frequency reconfigurable antenna using metasurface for wireless applications," presented at the 2015 International Conference on Innovations in Information, Embedded and Communication Systems (ICIIECS), 19-20 March 2015, 2015.

[4] N. Nguyen-Trong, L. Hall, and C. Fumeaux, "A Frequency- and Polarization-Reconfigurable Stub-Loaded Microstrip Patch Antenna," *IEEE Transactions on Antennas and Propagation,* vol. 63, no. 11, pp. 5235-5240, 2015.

[5] G. Lei and L. Kwai-Man, "Frequency-Reconfigurable Low-Profile Circular Monopolar Patch Antenna," *IEEE Transactions on Antennas and Propagation,* vol. 62, no. 7, pp. 3443-3449, 2014.

[6] R. Jeen-Sheen and T. Jia-Fu, "Frequency-Reconfigurable Microstrip Patch Antennas With Circular Polarization," *IEEE Antennas and Wireless Propagation Letters,* vol. 13, pp. 1112-1115, 2014.

[7] J. Costantine, Y. Tawk, S. E. Barbin, and C. G. Christodoulou, "Reconfigurable Antennas: Design and Applications," *Proceedings of the IEEE,* vol. 103, no. 3, pp. 424-437, 2015.

[8] W. Li *et al.*, "A Reconfigurable Polarization Converter Using Active Metasurface and Its Application in Horn Antenna," *IEEE Transactions on Antennas and Propagation,* vol. 64, no. 12, pp. 5281-5290, 2016.

[9] C. G. Christodoulou, Y. Tawk, S. A. Lane, and S. R. Erwin, "Reconfigurable Antennas for Wireless and Space Applications," *Proceedings of the IEEE,* vol. 100, no. 7, pp. 2250-2261, 2012.

[10] H. A. Majid, M. K. Abdul Rahim, M. R. Hamid, N. A. Murad, and M. F. Ismail, "Frequency-Reconfigurable Microstrip Patch-Slot Antenna," *IEEE Antennas and Wireless Propagation Letters,* vol. 12, pp. 218-220, 2013.

[11] A. F. Sheta and S. F. Mahmoud, "A Widely Tunable Compact Patch Antenna," *IEEE Antennas and Wireless Propagation Letters,* vol. 7, pp. 40-42, 2008.

[12] B. A. Cetiner, G. R. Crusats, L. Jofre, and N. Biyikli, "RF MEMS Integrated Frequency Reconfigurable Annular Slot Antenna," *IEEE Transactions on Antennas and Propagation,* vol. 58, no. 3, pp. 626-632, 2010.

[13] M. Gholamrezaei, F. Geran, and R. A. Sadeghzadeh, "Completely Independent Multi-Ultrawideband and Multi-Dual-Band Frequency Reconfigurable Annular Sector Slot Antenna (FR-ASSA)," *IEEE Transactions on Antennas and Propagation,* vol. 65, no. 2, pp. 893-898, 2017.

[14] S. L. S. Yang, A. A. Kishk, and K. F. Lee, "Frequency Reconfigurable U-Slot Microstrip Patch Antenna," *IEEE Antennas and Wireless Propagation Letters,* vol. 7, pp. 127-129, 2008.

[15] H.-Y. Li, C.-T. Yeh, J.-J. Huang, C.-W. Chang, C.-T. Yu, and J.-S. Fu, "CPW-Fed Frequency-Reconfigurable Slot-Loop Antenna With a Tunable Matching Network Based on Ferroelectric Varactors," *IEEE Antennas and Wireless Propagation Letters,* vol. 14, pp. 614-617, 2015.

[16] R. B. V. B. Simorangkir, Y. Yang, K. P. Esselle, and B. A. Zeb, "A Method to Realize Robust Flexible Electronically Tunable Antennas Using Polymer-Embedded Conductive Fabric," *IEEE Transactions on Antennas and Propagation,* vol. 66, no. 1, pp. 50-58, 2018.
[17] S. W. Cheung, Y. F. Cao, and T. I. Yuk, "Compact frequency reconfigurable slot antenna with continuous tuning range for cognitive radios," in *2015 9th European Conference on Antennas and Propagation (EuCAP)*, 2015, pp. 1-4.
[18] F. Costa, A. Monorchio, S. Talarico, and F. M. Valeri, "An Active High-Impedance Surface for Low-Profile Tunable and Steerable Antennas," *IEEE Antennas and Wireless Propagation Letters,* vol. 7, pp. 676-680, 2008.
[19] L. Bin, B. Sanz-Izquierdo, E. A. Parker, and J. C. Batchelor, "A Frequency and Polarization Reconfigurable Circularly Polarized Antenna Using Active EBG Structure for Satellite Navigation," *IEEE Transactions on Antennas and Propagation,* vol. 63, no. 1, pp. 33-40, 2015.
[20] W. Sam and Z. Zakaria, "The investigation of the varactor diode as tuning element on reconfigurable antenna," presented at the Antennas and Propagation (APCAP), 2016 IEEE 5th Asia-Pacific Conference on, 2016.
[21] A. Khidre, F. Yang, and A. Z. Elsherbeni, "A Patch Antenna With a Varactor-Loaded Slot for Reconfigurable Dual-Band Operation," *IEEE Transactions on Antennas and Propagation,* vol. 63, no. 2, pp. 755-760, 2015.
[22] L. Ge, M. Li, J. Wang, and H. Gu, "Unidirectional Dual-Band Stacked Patch Antenna With Independent Frequency Reconfiguration," *IEEE Antennas and Wireless Propagation Letters,* vol. 16, pp. 113-116, 2017.
[23] W. Liu, Z. N. Chen, and X. M. Qing, "Metamaterial-Based Low-Profile Broadband Mushroom Antenna," *IEEE Transactions on Antennas and Propagation,* vol. 62, no. 3, pp. 1165-1172, Mar 2014.
[24] W. Liu, Z. N. Chen, and X. M. Qing, "Metamaterial-Based Low-Profile Broadband Aperture-Coupled Grid-Slotted Patch Antenna," *IEEE Transactions on Antennas and Propagation,* vol. 63, no. 7, pp. 3325-3329, Jul 2015.
[25] S. X. Ta and I. Park, "Low-Profile Broadband Circularly Polarized Patch Antenna Using Metasurface," *IEEE Transactions on Antennas and Propagation,* vol. 63, no. 12, pp. 5929-5934, 2015.
[26] S. Chaimool, C. Rakluea, and P. Akkaraekthalin, "Low-profile unidirectional microstrip-fed slot antenna using metasurface," presented at the Intelligent Signal Processing and Communications Systems (ISPACS), 2011 International Symposium on, 2011.
[27] H. L. Zhu, X. H. Liu, S. W. Cheung, and T. I. Yuk, "Frequency-Reconfigurable Antenna Using Metasurface," *IEEE Transactions on Antennas and Propagation,* vol. 62, no. 1, pp. 80-85, 2014.
[28] H. L. Zhu, T. I. Yuk, and S. W. Cheung, "Mechanically pattern reconfigurable antenna using metasurface," *IET Microwaves, Antennas & Propagation,* vol. 9, no. 12, pp. 1331-1336, 2015.
[29] F. F. Araújo, A. G. D'Assunção, L. F. V. T. Costa, and W. S. Alves, "Design of rotatable metasurface microstrip antenna with reconfigurable polarization," presented at the Applied Computational Electromagnetics Society Symposium - Italy, 2017.
[30] S. Revathi, E. Sivakumar, and B. Ramachandran, "Metasurface based Circularly Polarized Reconfigurable Antenna," *Indian Journal of Science & Technology,* vol. 9, no. 44, 2016.
[31] Y.-M. Cai, Y. Yin, and K. Li, "A low-profile frequency reconfigurable metasurface patch antenna," presented at the Antennas and Propagation & USNC/URSI National Radio Science Meeting, 2017 IEEE International Symposium on, San Diego, CA, USA, 2017.
[32] SMV1405 Varactors Datasheet [Online]. Available: www.skyworksinc.com
[33] F. Costa, O. Luukkonen, C. R. Simovski, A. Monorchio, S. A. Tretyakov, and P. M. de Maagt, "TE Surface Wave Resonances on High-Impedance Surface Based Antennas: Analysis and Modeling," *IEEE Transactions on Antennas and Propagation,* vol. 59, no. 10, pp. 3588-3596, Oct 2011.

YUAN-MING CAI received the B.S. degree in electronic information engineering and the Ph.D. degree in electromagnetic wave and microwave technology from Xidian University, Xi'an, China, in 2011 and 2016, respectively.

He is currently a Lecturer with the National key Laboratory of Science and Technology on Antennas and Microwaves, Xidian University, Xi'an, China. His research interests include multiband and wideband antennas, circularly polarized antennas, and reconfigurable antennas.

KE LI received the B.S. degree in electronic information engineering and the Ph.D. degree in electromagnetic wave and microwave technology from Xidian University, Xi'an, China, in 2011 and 2016, respectively.

She is currently a Lecturer with the School of Information Science and Technology, Northwest University, Xi'an, China. Her research interests include multiband antenna design, reconfigurable antennas, and metamaterials.

YINGZENG YIN received the PhD degree in electromagnetic wave and microwave technology from Xidian University, Xi'an, China, in 2002, respectively. From 1990 to 1992, he was a Research Assistant and an Instructor at the institute of antennas and electromagnetic scattering, Xidian University. From 1992 to 1996, he was an associate professor in the Department of Electromagnetic Engineering, Xidian University. Since 2004, he has been a Professor at Xidian University.

His research interests include design of microstrip antennas, artificial magnetic conductors, phased array antennas, and computer aided design for antennas.

STEVEN GAO received the Ph.D. degree in microwave engineering from Shanghai University, Shanghai, China, in 1999.

He is currently a Professor and the Chair of RF and microwave engineering with the University of Kent, Canterbury, U.K. He has authored more than 250 papers and co-authored two books including Space Antenna Handbook (Wiley, 2012) and Circularly Polarized Antennas (IEEE-Wiley, 2014), and holds several patents in smart antennas and RF. His current research interests include smart antennas, phased arrays, satellite antennas, RF/microwave/millimeterwave/terahertz circuits, satellite communications, ultra-wideband radars, synthetic-aperture radars, and mobile communications.

WEI HU received the B.S. degree in electronic information engineering and the Ph.D. degree in electromagnetic fields and microwave technology from Xidian University, Xi'an, China, in 2008 and 2013, respectively.

He is currently an Associate Professor with the National Key Laboratory of Antennas and Microwave Technology, Xidian University. His current research interests include multiband and wideband antennas, circularly polarized, and dual-polarized antennas, and multi-in multi-out technologies.

LUYU ZHAO received the B.Eng. degree from Xidian University, Xi'an, China in 2007, and the Ph. D. degree from The Chinese University of Hong Kong, Shatin, Hong Kong in 2014.

He is currently an associate professor at the National Key Laboratory of Antennas and Microwave Technology, Xidian University since 2016.

From 2007 to 2009, he was with the Key Laboratory of Antennas and Microwave Technology, Xidian University, as a Research Assistant, where he was involved with software and hardware implementation of RF identification (RFID) technologies. From 2014 to 2015, he was a Postdoctoral Fellow at The Chinese University of Hong Kong, Shatin, Hong Kong. From Oct. 2015 to Oct. 2016, he was with Wyzdom Wireless Co. Ltd., where he was a co-founder and CTO.

His current research interests include design and application of multiple antenna systems for next generation mobile communication systems, innovative passive RF and microwave components and systems, millimeter wave and terahertz antenna array, meta-material based or inspired antenna arrays.

Dr. Zhao was the recipient of the Best Student Paper Award in 2013 IEEE 14th HK AP/MTT Postgraduate Conference. The Honorable Mention Award of 2017 Asia-Pacific Conference on Antenna and Propagation.